18èmes Journées Internationales de Thermique (JITH 2017)
Monastir (Tunisie), 25 - 27 Octobre 2017

Thermal analysis of latent thermal energy storage module using multiple phase change materials having different melting temperatures

Fouzi BENMOUSSA[*1], Hocine BENMOUSSA[1], Ahmed BENZAOUI[2]

[1]Faculty of Technology, Mechanics Department, University of Batna-2, Batna, Algeria
[2]Faculty of Physics, University of Sciences and Technology Houari Boumedienne, Algiers, Algeria
E-mail: ***benmoussa_fouzi@yahoo.fr****; hocine_b@hotmail.com; a1benzaoui@yahoo.fr*

Abstract
In this paper, the latent thermal energy storage (LTES) module of the horizontal shell-and-tube type is numerically analyzed. The LTES module consists of an inner tube, an outer tube and an annulus filled with three different phase change materials (PCMs) named PCM1, PCM2 and PCM3, having different melting temperatures (338 K, 323 K and 308 K, respectively), water is used as heat transfer fluid (HTF). The effects of the HTF inlet temperature on the unsteady temperature and melting fraction evolution of each PCM as well as the unsteady total energy stored evolution in different zone of PCMs are determined. Numerical results show that, melting rate of PCM3 is the fastest and that of PCM1 is the slowest, the unsteady temperature evolution of PCM3 change quickly compared to PCM1. The whole LTES melting process can be divided into three periods for the change of melting fraction. Numerical results indicate also that, heat storage capacity is large when the temperature difference between the HTF inlet temperature and the melting point of PCMs is large.

Keywords: Latent thermal energy storage; phase change material; Heat charging; Melting fraction; Numerical simulation.

1. Introduction

A lot of efforts and researches on the utilization of solar energy have been carried out due to the globe energy crisis, global warming and environmental pollution. These efforts include solar buildings (Xiao et al.[1], Kuznik et al.[2]), solar water heating systems (Garnier et al.[3], Sutthivirode et al.[4]) and solar energy generation systems (Yang et al.[5], Tao et al.[6]). However, solar energy has a serious shortcoming that it is unstable and discontinuous with different weathers, times and seasons. To ensure the solar energy system operations continuously, thermal energy storage become a necessary component. The main objective is then to eliminate the mismatch between energy supply and energy demand.
The latent thermal energy storage (LTES) using phase change materials (PCMs) have been relevant, especially in solar thermal applications. Solid–liquid phase change provides considerable advantages such as high storage capacity and nearly isothermal behavior during charging process. Therefore, LTES with single and multiple PCMs under shell-and-tube unit have gained considerable attention worldwide recently. Lacroix [7] developed a 2D numerical model to analyse the thermal behavior of a cylindrical storage system with n-octadecane as PCM and water as heat transfer fluid (HTF). A series of numerical experiments are also undertaken to assess the effects of various thermal and geometric parameters on the heat transfer process and on the behavior of the system. Wang et al. [8] numerically studied the effects of temperature difference between the HTF inlet temperature and melting point of PCM, the HTF inlet mass flow rate on heat charging and heat discharging

performance of a shell-and-tube unit using n-octadecane as PCM. The results show that HTF inlet temperature has great effect on the time to complete heat charging or discharging process. Tao et al. [9] investigated the performance of high temperature molten salt LTES unit under variable conditions, the effects of HTF inlet temperature, velocity and tube geometric parameters on melting time, melting fraction and heat storage rate. The results show that within the studied parameters, the HTF inlet temperature has the largest effect on heat storage rate. Ait Adine and El Qarnia [10] presented a numerical study of a LTES unit consisting of a shell-and-tube type filled with two PCMs, P116 and n-octadecane. Numerical results indicated that there is an optimum proportion between multiple PCMs to obtain the maximum thermal energy charging in the storage unit. Akgun et al. [11] analyzed the LTES unit of the shell-and-tube type with three kinds of paraffin as PCMs. A novel tube-in-shell storage geometry was introduced and the effects of the Reynolds and Stefan numbers on the melting and solidification behaviors were examined. Fang and Chen [12] presented a theoretical model for the performance of a shell-and-tube LTES unit using multiple PCMs. Numerical simulations are carried out to investigate the effects of different multiple PCMs on the melted fraction, stored thermal energy and fluid outlet temperature. Li et al. [13] developed a mathematical model of a shell-and-tube LTES unit of three kinds of PCMs having different high melting point for solar thermal power, air is used as HTF. Instantaneous solid-liquid interface positions, liquid fractions and melting times of each PCM have been obtained by a series of numerical calculations and represented graphically.

The LTES unit analysed in this paper is a shell-and-tube type of heat exchanger with three kinds of PCMs, named PCM1, PCM2 and PCM3, having the same thermo-physical characteristics, except their melting temperature, water is used as HTF. In order to study the thermal behavior of the unit in term of unsteady temperature and melting fraction evolution of each PCM, as well as the unsteady total energy stored evolution in different zone of PCMs, a mathematical model based on the conservation energy equations was developed and numerically investigated. Charging process was studied numerically under three different HTF inlet temperatures above the melting point of the PCM1. Calculation of the unsteady temperature and melting fraction evolution of each PCM and the total energy stored under variable HTF inlet temperatures were necessary for evaluating the overall thermal performance of the unit.

2. Physical model and governing equations

2.1. Physical model

The shell-and-tube LTES unit considered in the present study is shown in Figure 1a. It consists of an inner tube, an outer tube and an annulus filled with three kinds of PCMs, paraffin wax named PCM1, PCM2 and PCM3, having different melting temperatures (338 K, 323 K and 308 K, respectively). The two-dimension physical model to be analysed is shown in Figure 1b. The length for the computation domain (L_1=L_2=L_3) is 0.33 m, the radius for the inner tube (R_1) is 0.635 cm, and the radius for the shell side (R_2) is 1.29 cm. The multiple PCMs have the same thermo-physical characteristics, except their melting temperatures. The thermo-physical property of PCMs is summarized in Table 1. The initial temperature of PCMs was set at 15 K below the melting point of PCM3. HTF, water, flows through the inner tube and exchanges heat with PCMs. Charging process is studied numerically under three different HTF inlet temperatures above the melting point of the PCM1 (343 K, 348 K and 358 K). The HTF mass flow rate was maintained constant during the numerical tests to a value of 6.10^{-3} kg/s, which correspond to water velocity 0.05 m/s. Table 2 summarizes the thermo-physical properties of HTF.

2.2. Assumptions

In order to simplify the physical and mathematical model, the following assumptions are adopted.

1) The HTF is incompressible and can be considered as a newtonian fluid;
2) The HTF flow is laminar, HTF inlet temperature and inlet velocity are both constant;
3) The thermo-physical properties of the HTF and PCMs are constant;
4) The effect of liquid PCMs natural convection is negligible;
5) Initial temperature of the unit is uniform, the PCMs are in solid phase during charging process;
6) The problem is axisymmetric;

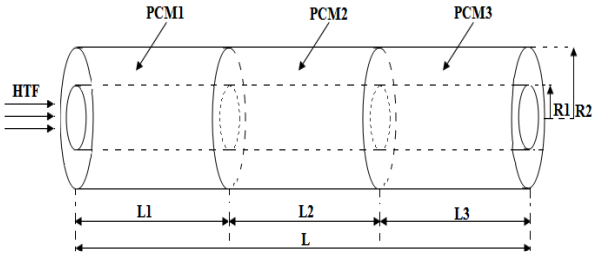

Figure 1a: Schematic representation of shell-and-tube PCMs storage unit.

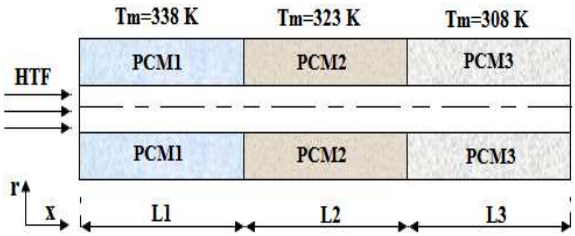

Figure 1b: Physical model for numerical calculations.

Table1: Thermo-physical properties of the paraffin types considered in the study

	T_M *(K)*	ρ *(Kg. m^{-3})*	k *(W. $m^{-1}K^{-1}$)*	Cp *(J. $kg^{-1}K^{-1}$)*	ΔH *(J. kg^{-1})*	μ *(Kg. $m^{-1}s^{-1}$)*
PCM1	338	800	0.2	2000	255.10^3	4.10^{-3}
PCM2	323	800	0.2	2000	255.10^3	4.10^{-3}
PCM3	308	800	0.2	2000	255.10^3	4.10^{-3}

Table 2: Thermo-physical properties of HTF (Incropera et al. [14])

Charging process	ρ *(Kg. m^{-3})*	k *(W. $m^{-1}K^{-1}$)*	Cp *(J. $kg^{-1}K^{-1}$)*	μ *(Kg. $m^{-1}s^{-1}$)*
T=343 K	976	0.668	4191	389.10^{-6}
T=348 K	973	0.668	4195	365.10^{-6}
T=358 K	967	0.674	4203	324.10^{-6}

2.3. Governing equations

The LTES process in the shell-and-tube unit can be treated as an axisymmetric model, the unit is divided into the following four subsections: (1) HTF flow in the tube; (2) three sections filled by three different PCMs. Consequently, the energy equations for the HTF and PCMs are shown as follows.

2.3.1. For the HTF region, $x \succ 0,\ \ 0 \prec r \prec R_1,\ \ t \succ 0$

$$\left(\rho C_p\right)_f \left(\frac{\partial T_f\left(x,r,t\right)}{\partial t} + U_f \frac{\partial T_f\left(x,r,t\right)}{\partial x} \right) = k_f \left(\frac{\partial^2 T_f\left(x,r,t\right)}{\partial r^2} + \frac{1}{r}\frac{\partial T_f\left(x,r,t\right)}{\partial r} + \frac{\partial^2 T_f\left(x,r,t\right)}{\partial x^2} \right) \quad (1)$$

Where ρ is the density of fluid, C_p the specific heat, U the fluid velocity and k is the thermal conductivity

2.3.2. For the PCMs region, $x \succ 0,\ \ R_1 \prec r \prec R_2,\ \ t \succ 0$

$$\left(\rho C_p\right)_{pcm} \frac{\partial \theta_{pcm}\left(x,r,t\right)}{\partial t} = k_{pcm} \left(\frac{\partial^2 \theta_{pcm}\left(x,r,t\right)}{\partial x^2} + \frac{1}{r}\frac{\partial}{\partial r}\left(r \frac{\partial \theta_{pcm}\left(x,r,t\right)}{\partial r} \right) \right) - \rho_{pcm} \Delta H \frac{\partial f}{\partial t} \quad (2)$$

$$\theta_{pcm} = \left(T - T_M\right),\ T_M = \begin{cases} T_{M1} & 0 \le x \le L_1 \\ T_{M2} & L_1 \le x \le L_2 \\ T_{M3} & L_2 \le x \le L_3 \end{cases} \quad (3)$$

f is the PCMs melting fraction. The melting fraction is determined as:

$$\begin{Bmatrix} f = 0, & \theta \prec 0 & Solid \\ 0 \prec f \prec 1, & \theta = 0 & Solid + Liquid \\ f = 1, & \theta \succ 0 & Liquid \end{Bmatrix} \quad (4)$$

The Eq. (2) is formulated by using the enthalpy method (Voller [15]), in which the total enthalpy is split into sensible heat and latent heat:

$$H(T) = h(T) + \rho\, f\, \Delta H \quad (5)$$

$$\text{Where: } h(T) = \int_{T_M}^{T} \rho C_p dT \quad (6)$$

2.4. Initial and boundary conditions

2.4.1. Initial conditions

For the PCMs region:

$$T_{PCM1} = T_{PCM2} = T_{PCM3}\left(x, R_1 \le r \le R_2, t = 0\right) = 293\,K \quad (7a)$$

2.4.2. Boundary conditions

For the HTF region:

$$\begin{cases} T_f\left(0, 0 \le r \le R_1, t\right) = T_{f,in} \\ U_f\left(0, 0 \le r \le R_1, t\right) = U_{f,in} = 0.05\,m/s \end{cases} \quad (8a)$$

$$\left.\frac{\partial U_f(x,r,t)}{\partial r}\right|_{r=0} = \left.\frac{\partial T_f(x,r,t)}{\partial r}\right|_{r=0} = 0 \quad (8b)$$

For the PCMs region:

$$\left.\frac{\partial \theta_{pcm}(x,r,t)}{\partial r}\right|_{r=R_2} = 0 \quad (8c)$$

$$\left.\frac{\partial \theta_{pcm1}(x,r,t)}{\partial x}\right|_{x=0} = \left.\frac{\partial \theta_{pcm3}(x,r,t)}{\partial x}\right|_{x=L3} = 0 \quad (8d)$$

$$k_{pcm1}\left.\frac{\partial \theta_{pcm1}(x,r,t)}{\partial x}\right|_{x=L1} = k_{pcm2}\left.\frac{\partial \theta_{pcm2}(x,r,t)}{\partial x}\right|_{x=L1} \quad (8e)$$

$$k_{pcm2}\left.\frac{\partial \theta_{pcm2}(x,r,t)}{\partial x}\right|_{x=L2} = k_{pcm3}\left.\frac{\partial \theta_{pcm3}(x,r,t)}{\partial x}\right|_{x=L2} \quad (8f)$$

At the inner surface boundary:

$$h_f\left(\theta_f - \theta(x, r = R_1, t)\right) = -k_{pcm}\left.\frac{\partial \theta_{pcm}(x,r,t)}{\partial r}\right|_{r=R1} \quad (8g)$$

Where h is local convective heat transfer coefficient *(W.m^2.K^{-1})*

The total energy stored capacity for each zone of PCM during charging process of the LTES unit can be represented by the following expression:

$$E_{PCM} = \int_{T_{PCM}}^{T_M} (mC_p)_{PCM}\, dT + (m\Delta H)_{PCM}\ f + \int_{T_{PCM}}^{T_{f,in}} (mC_p)_{PCM}\, dT \quad (9)$$

The first term of the Eq. (9) represents the sensible heat charging period, when each PCM temperature increase from its initial temperature to the phase change. The second term represents the latent heat charging during the phase change period. The third term represents the second sensible heat charging period under a fusion form until reaching the steady state.

3. Simulation model

3.1. Numerical Computations

For the computational procedure, the two-dimension geometric model of the phase change LTES unit is drawn and meshed in the software Gambit with uniform grid size. Then, the numerical computations are performed by adopting commercial CFD code Fluent 6.3.26, which employs the finite volume method described by Patankar [16]. The energy equations were discretized with the first order upwind scheme. The time integration has been performed fully implicitly and control volumes of a uniform size and constant time steps were used. The grid size used in this study was 100 (axial) × 20 (radial) and the time step was 5 s.

4. Results and discussion

The thermal analysis of the shell-and-tube LTES including three kinds of PCMs having different melting temperature is presented in this section. A large set of numerical tests have been conducted in order to analyze the heat transfer process inside the unit under the influence of different HTF inlet temperatures. The time wise variation of the temperature and melting fraction respecting to time at locations T_1 *(x=16.5, r=0.99) cm* inside PCM1, T_2 *(x=51, r=0.99) cm* inside PCM2 and T_3 *(x=82.5, r=0.99) cm* inside PCM3 as well as the variation of total energy stored in different zone of PCMs have been obtained by a series of numerical calculations and represented graphically.

4.1. Unsteady temperature evolution of PCM1, PCM2 and PCM3

Under the same HTF inlet velocity and three different HTF inlet temperatures, the PCMs temperature evolution at some typical points (T_1, T_2, and T_3) along the axial direction at r= 0.99 cm position are shown in Figures 2(a-b-c).

As shown in Figures 2(a-b-c), it can be clearly observed the transient thermal behavior of the LTES unit which presents three distinct periods. During the first period, an increasing of temperature of each PCM was observed during this period from the start of charging process until the beginning of the phase change, corresponding to the melting point of each PCM, the three kinds of PCMs stores energy primarily by sensible heat. During the second period, the thermal energy is mainly charged by latent heat, and the temperature evolution of each PCM keeps constant for a period of time. At the third period, each PCM temperature starts to increase again, reaches its maximum value, then remains constant and equals to the HTF inlet temperature. During this period, the energy is charged only by sensible heat under a fusion form.

It can be seen that, the melting rate of PCM3 is the fastest and that of PCM1 is the slowest for all three different HTF inlet temperatures. The PCM3 temperature evolution increases rapidly with time passing through the phase change period until reaching the steady state, which can be explained by the fact that the melting point of PCM3 (T_{M3}= 308 K) is lower than PCM1 (T_{M1}= 338 K), so their temperature reach quickly their melting point before PCM1, then enter to the second period. It is also found that, for high HTF inlet temperature the charging process is rapidly reached for the three kinds of PCMs.

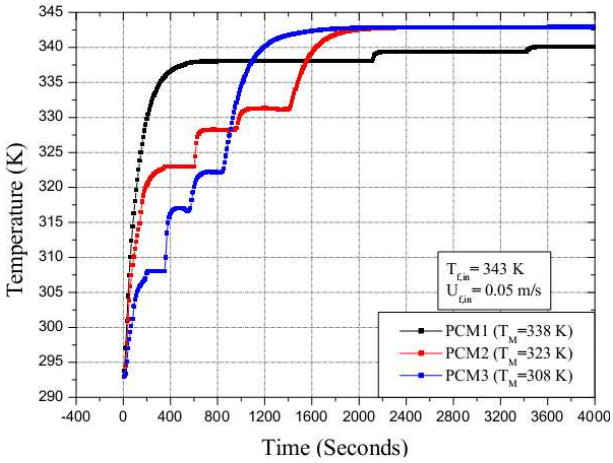

Figure 2a: Unsteady temperature evolution of PCM1, PCM2 and PCM3 ($T_{f,in}$ =343 K).

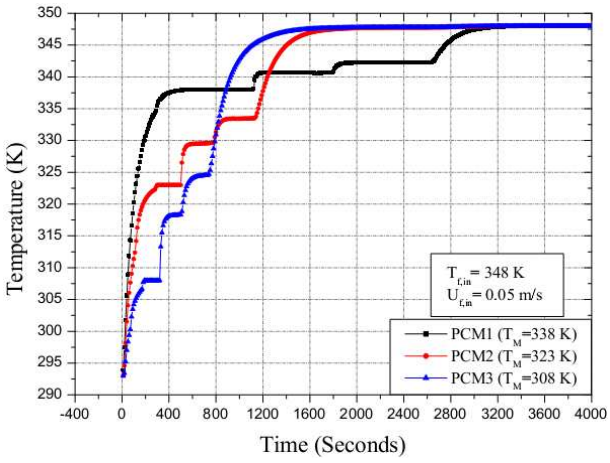

Figure 2b: Unsteady temperature evolution of PCM1, PCM2 and PCM3 ($T_{f,in}$ =348 K).

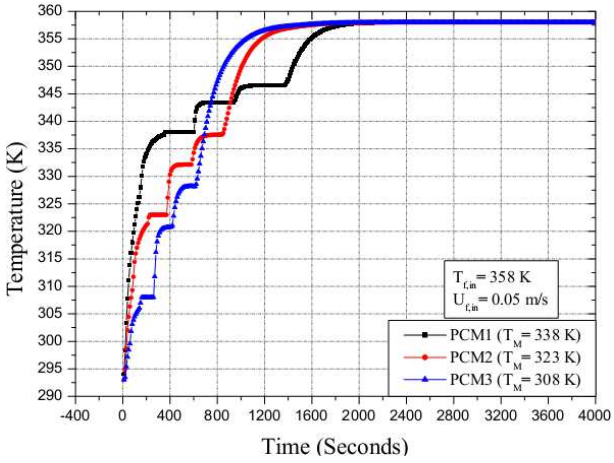

Figure 2c: Unsteady temperature evolution of PCM1, PCM2 and PCM3 ($T_{f,in}$ =358 K).

4.2. Unsteady melting fraction evolution of PCM1, PCM2 and PCM3

Figures 3(a-b-c) display the unsteady melting fraction evolution of PCM1, PCM2 and PCM3, under three different HTF inlet temperatures. From the figures, it can be seen that the whole LTES charging process can be divided into three periods. The first is sensible heat charging (SHC) period, where the PCMs temperature is lower than their melting point, each PCM keeps solid phase and their melting fraction is zero. The second is latent heat charging (LHC) period, where the PCMs temperature reach their melting point and keeps constant; this period will be ongoing until all the PCMs are melted, and the corresponding melting fraction increases from zero to one. The third is sensible heat charging too, where each PCM temperature is larger than their melting point and the PCMs keeps liquid phase, until the heat charging process is over, during this period the melting fraction keeps at one.

Compared to PCM1, the PCM3 melting fraction changes rapidly with time during the heating process passing through the phase change period until reaching the steady state. The same point of explanation we can notice concerning the low melting point of PCM3, which make the temperature and melting fraction evolution change rapidly with time. Also when the HTF inlet temperature increases, the temperature difference between the HTF and PCMs augments which increases the heat transfer rates for PCM1, PCM2 and PCM3; more energy is transmitted firstly to PCM3, PCM2 then to PCM1, which make the first SHC and LHC periods for all three PCMs shortened. The effects of increasing in HTF inlet temperature on the SHC and LHC periods for PCMs are different; it's very remarkable in PCM1 with high melting temperature.

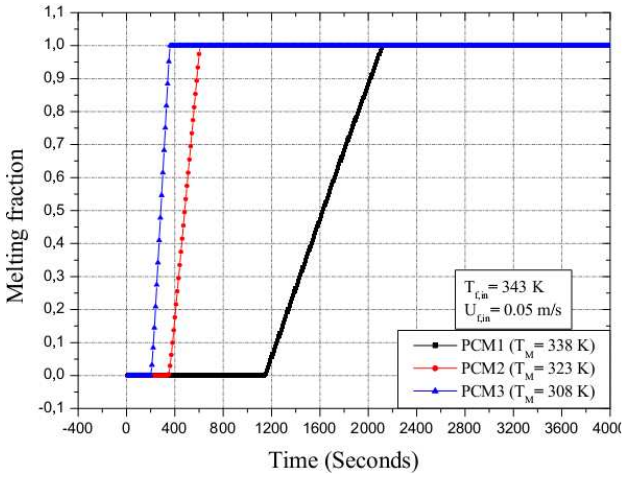

Figure 3a: Unsteady melting fraction evolution of PCM1, PCM2 and PCM3 ($T_{f,in}$ =343 K).

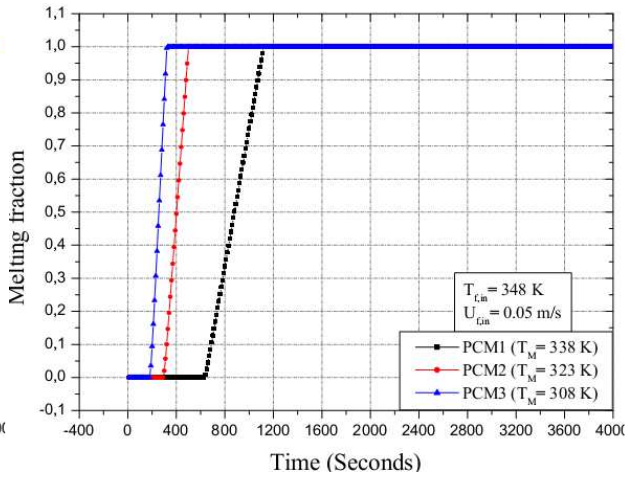

Figure 3b: Unsteady melting fraction evolution of PCM1, PCM2 and PCM3 ($T_{f,in}$ =348 K).

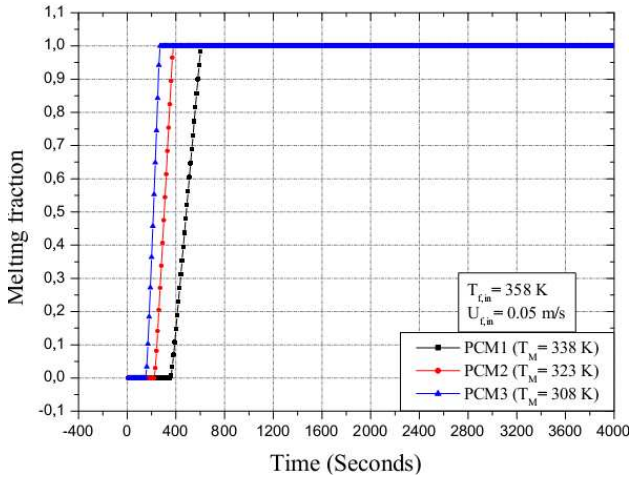

Figure 3c: Unsteady melting fraction evolution of PCM1, PCM2 and PCM3 ($T_{f,in}$ =358 K).

4.3. Unsteady total energy stored evolution in different zone of PCMs

The unsteady total energy stored evolution in different zone of PCMs for three different HTF inlet temperatures are shown in Figures 4(a-b-c), the HTF inlet velocity was maintained constant during the numerical tests.

For a given HTF inlet temperature, the total energy stored gradually increase from minimum value which define the beginning of the first SHC period to maximum value defined the end of the second SHC period. The final amount of total energy stored by each PCM is the same, except the time needed for completing the charging process; this period of time depends on the melting point of each PCM, for PCM with high melting point, the time period to complete the charging process is longer than for PCM with low melting point. Under HTF inlet temperature 348 K, the time period to complete the charging process when the total energy stored keep a fixed value is within 3270 s, 1600 s and 1200 s for PCM1, PCM2 and PCM3, respectively. When the HTF inlet temperature increases, the thermal energy carried by the HTF enhances, then, the heat transmitted to the PCMs becomes important and the charging process for all PCM is rapidly reached. The results show also that, heat storage capacity is large when the temperature difference between the HTF inlet temperature and the melting point of PCMs is large. The final amount of total energy stored by each PCM is within 344000 J/Kg, 354000 J/Kg and 374000 J/Kg for HTF inlet temperature 343 K, 348 K and 358 K.

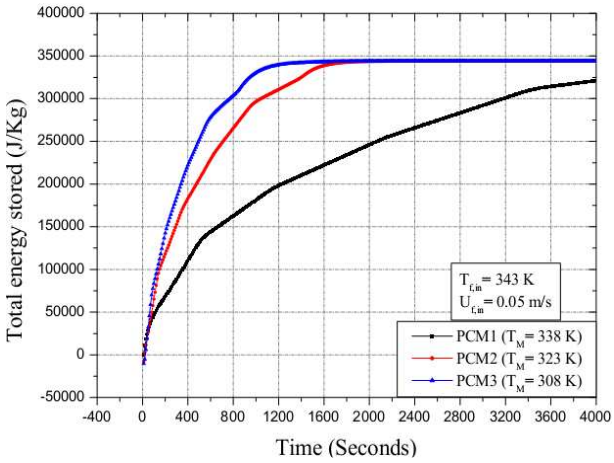

Figure 4a: Unsteady total energy stored evolution in PCM1, PCM2 and PCM3 ($T_{f,in}$ =343 K).

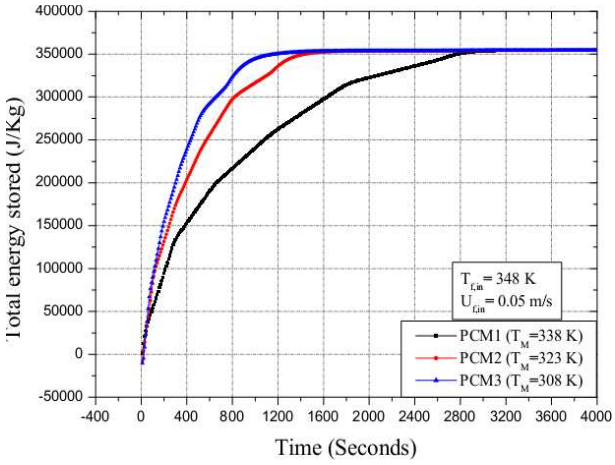

Figure 4b: Unsteady total energy stored evolution in PCM1, PCM2 and PCM3 ($T_{f,in}$ =348 K).

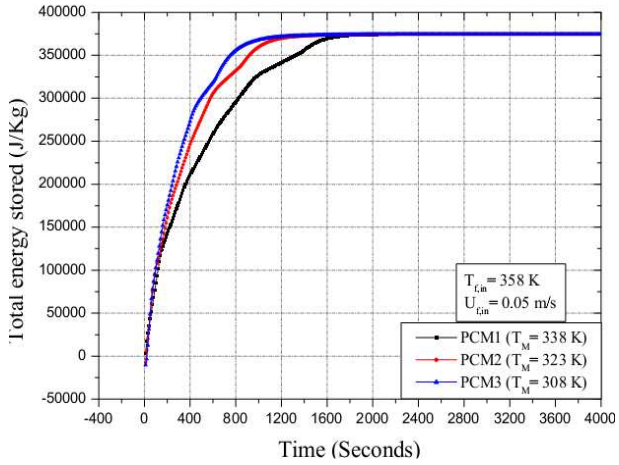

Figure 4c: Unsteady total energy stored evolution in PCM1, PCM2 and PCM3 ($T_{f,in}$ =358 K).

Conclusion

A thermal analysis of a LTES unit using shell-and-tube type, tested with three kinds of PCMs having different melting temperatures have been studied numerically. A mathematical model formulated in two-dimensional cylindrical coordinates based on the energy equations was developed. The effects of the HTF inlet temperature on the thermal behavior of the unit in term of PCMs temperature and melting fraction evolution as well as the unsteady total energy stored evolution in different zone of PCMs have been obtained by a series of numerical calculations and represented graphically. According to the results and discussions, the following conclusions can be derived:

1) Melting rate of PCM3 is the fastest and that of PCM1 is the slowest, the unsteady temperature and melting fraction evolution of PCM3change quickly compared to PCM1;
2) The whole LTES melting process can be divided into three periods for the change of melting fraction regarding to time in each PCM;
3) Charging process is rapidly reached for high temperature difference between HTF inlet temperature and melting point of PCMs;
4) The effects of the HTF inlet temperature on the total energy stored show that heat storage capacity is large for high HTF inlet temperature.

Nomenclature

Symbole		Symboles grecs	
C_p	Specific heat, *J/kg. K*	f	PCM melting fraction
E	Total energy stored, *J/kg*	μ	Dynamic viscosity, $Kg.m^{-1}s^{-1}$
k	Thermal conductivity, *W/m. K*	ρ	Density, $Kg.m^{-3}$
m	Mass of the PCMs, *Kg*	ΔH	Latent heat of fusion, $KJ.kg^{-1}$
R_1	Inner tube radius, *m*	$\theta=(T-T_M)$	Relative temperature, *K*
R_2	Outer tube radius, *m*		
r	Radial coordinate, *m*	Exposant, Indices	
T	Temperature, *K*	f	Heat transfer fluid
t	Time, *s*	pcm	Phase change material
U	Velocity, *m/s*	M	Melting point of PCMs
x	Axial coordinate, *m*	in	Inlet boundary
		ini	Initial condition

Références

[1] W. Xiao, X. Wang and Y.P. Zhang, Analytical optimization of interior PCM for energy storage in a light weight passive solar room, *Applied Energy*, Volume 86, Pages 2013-2018, 2009.

[2] F. Kuznik and J. Virgone, Experimental assessment of a phase change material for wall building use, *Applied Energy*, Volume 86, Pages 2038-2046, 20019.

[3] C. Garnier, J. Currie and T. Muneer, Integrated collector storage solar water heater: temperature stratification, *Applied Energy*, Volume 86, Pages 1465-1469, 2009.

[4] K. Sutthivirode, P. Namprakai and N. Roonprasang, A new version of a solar water heating system coupled with a solar water pump, *Applied Energy*, Volume 86, Pages 1423-1430, 2009.

[5] Z. Yang and S.V. Garimella, Molten-salt thermal energy storage in thermoclines under different environmental boundary conditions, *Applied Energy*, Volume 87, Pages 3322-3329, 2010.

[6] Y.B. Tao and Y.L. He, Numerical study on coupled fluid flow and heat transfer process in parabolic trough solar collector tube, *Solar Energy*, Volume 84, Pages 1863-1872, 2010.

[7] M. Lacroix, Numerical simulation of a shell-and-tube latent heat thermal energy storage unit, *Solar Energy*, Volume 50, Pages 357-367, 1993.

[8] W.W. Wang, K. Zhang, L.B. Wang and Y.L. He, Numerical study of the heat charging and discharging characteristics of a shell-and-tube phase change heat storage unit, *Applied Thermal Engineering*, Volume 58, Pages 542-553, 2013.

[9] Y.B. Tao, M.J. Li, Y.L. He and W.Q. Tao, Effects of parameters on performance of high temperature molten salt latent heat storage unit, *Applied Thermal Engineering*, Volume 72, Pages 48-55, 2014.

[10] H. Ait Adine and H. El Qarnia, Numerical analysis of the thermal behaviour of a shell-and-tube heat storage unit using phase change materials, *Applied Mathematical Modelling*, Volume 33, Pages 2132-2144, 2009.

[11] M. Akgun, O. Aydin and K. Kaygusuz, Thermal energy storage performance of paraffin in a novel tube-in-shell system, *Applied Thermal Engineering*, Volume 28, Pages 405-413, 2008.

[12] M. Fang and G. Chen, Effects of different multiple PCMs on the performance of a latent thermal energy storage system, *Applied Thermal Engineering*, Volume 27, Pages 994-1000, 2007.

[13] Y.Q Li, Y.L He, H.J Song, C Xu and W.W Wang, Numerical analysis and parameters optimization of shell-and-tube heat storage unit using three phase change materials, *Renewable Energy*, Volume 59, Pages 92-99, 2013.

[14] F.P. Incropera, D.P. Dewitt, T.L. Bergman and A.S. Lavine, Fundamentals of heat and mass transfer, Sixth edition, *Wiley*, New York 1996.

[15] V.R. Voller, Fast implicit finite-difference method for the analysis of phase change problems, *Numerical Heat Transfer*, Volume 17, Pages 155-169, 1990.

[16] S.V. Patankar, Numerical Heat Transfer and Fluid Flow, *Hemisphere Publishing Corporation*, New York, 1980.